Optical properties of ordered vertical arrays of multi-walled carbon nanotubes from FDTD simulations

Hua Bao, Xiulin Ruan*, and Timothy S. Fisher

School of Mechanical Engineering, Birck Nanotechnology Center, and Energy Center
Purdue University, West Lafayette, Indiana 47907-2088

*ruan@purdue.edu

Abstract: A finite-difference time-domain (FDTD) method is used to model thermal radiative properties of vertical arrays of multi-walled carbon nanotubes (MWCNT). Individual CNTs are treated as solid circular cylinders with an effective dielectric tensor. Consistent with experiments, the results confirm that CNT arrays are highly absorptive. Compared with the commonly used Maxwell-Garnett theory, the FDTD calculations generally predict larger reflectance and absorbance, and smaller transmittance, which are attributed to the diffraction and scattering within the cylinder array structure. The effects of volume fraction, tube length, tube distance, and incident angle on radiative properties are investigated systematically. Low volume fraction and long tubes are more favorable to achieve low reflectance and high absorbance. For a fixed volume fraction and finite tube length, larger periodicity results in larger reflectance and absorbance. The angular dependence studies reveal an optimum incident angle at which the reflectance can be minimized. The results also suggest that an even darker material could be achieved by using CNTs with good alignment on the top surface.

OCIS codes: (310.6628) Subwavelength structures, nanostructures.

References and links

1. W. Z. Li, S. S. Xie, L. X. Qian, B. H. Chang, B. S. Zou, W. Y. Zhou, R. A. Zhao, and G. Wang, "Large-scale synthesis of aligned carbon nanotubes," Science **274**, 1701–1703 (1996).
2. G. L. Zhao, D. Bagayoko, and L. Yang, "Optical properties of aligned carbon nanotube mats for photonic applications," J. Appl. Phys. **99**, 114311 (2006).
3. K. Kempa, B. Kimball, J. Ryhczynski, Z. P. Huang, P. F. Wu, D. Steeves, M. Sennett, M. Giersig, D. V. G. L. N. Rao, D. Carnahan, D. Z. Wang, J. Y. Lao, W. Z. Li, and Z. F. Ren, "Photonic crystals based on periodic arrays of aligned carbon nanotubes," Nano Lett. **3**, 13–18 (2003).
4. E. Lidorikis and A. C. Ferrari, "Photonics with multiwall carbon nanotube arrays," ACS Nano **3**, 1238–1248 (2009).
5. G. Y. Slepyan, M. V. Shuba, and S. A. Maksimenko, "Theory of optical scattering by achiral carbon nanotubes and their potential as optical nanoantennas," Phys. Rev. B **73**, 195416 (2006).
6. K. Kempa, J. Ryhczynski, Z. P. Huang, K. Gregorczyk, A. Vidan, B. Kimball, J. Carlson, G. Benham, Y. Wang, A. Herczynski, and Z. F. Ren, "Carbon nanotubes as optical antennae," Adv. Mater. **19**, 421–426 (2007).
7. X. J. Wang, J. D. Flicker, B. J. Lee, W. J. Ready, and Z. M. Zhang, "Visible and near-infrared radiative properties of vertically aligned multi-walled carbon nanotubes," Nanotechnology **20**, 215704 (2009).
8. Y. Wang, K. Kempa, B. Kimball, J. B. Carlson, G. Benham, W. Z. Li, T. Kempa, J. Rybczynski, A. Herczynski, and Z. F. Ren, "Receiving and transmitting light-like radio waves: Antenna effect in arrays of aligned carbon nanotubes," Appl. Phys. Lett. **85**, 2607 (2004).

#122794 - $15.00 USD Received 15 Jan 2010; revised 23 Feb 2010; accepted 3 Mar 2010; published 12 Mar 2010

9. S. Shoji, H. Suzuki, R. P. Zaccaria, Z. Sekkat, and S. Kawata, "Optical polarizer made of uniaxially aligned short single-wall carbon nanotubes embedded in a polymer film," Phys. Rev. B, 153407 (2008).
10. Z.-P. Yang, L. Ci, J. A. Bur, S.-Y. Lin, and P. M. Ajayan, "Experimental observation of extremely dark material made by a low-density nanotube array," Nano Lett. **8**, 446 (2008).
11. K. Mizuno, J. Ishii, H. Kishida, Y. Hayamizu, S. Yasuda, D. N. Futaba, M. Yumura, and K. Hata, "A black body absorber from vertically aligned single-walled carbon nanotubes," Proc. Natl. Acad. Sci. USA **106**, 6044–6047 (2008).
12. M. F. Lin, "Plasmons and optical properties of carbon nanotubes," Phys. Rev. B **50**, 17744 (1994).
13. S. M. Bachilo, M. S. Strano, C. Kittrell, R. H. Hauge, R. E. Smalley, and R. B. Weisman, "Structure-assigned optical spectra of single-walled carbon nanotubes," Science **298**, 2361–2366 (2002).
14. G. Y. Guo, K. C. Chu, D. S. Wang, and C. G. Duan, "Linear and nonlinear optical properites of carbon nanotubes from first-principles calculations," Phys. Rev. B **69**, 205416 (2004).
15. M. F. Lin, "Optical spectra of single-wall carbon nanotube bundles," Phys. Rev. B **62**, 13153 (2000).
16. L. Tsakalakos, J. Balch, J. Fronheiser, B. A. Korevaar, O. Sulima, and J. Rand, "Silicon nanowire solar cells," Appl. Phys. Lett. **91**, 233117 (2007).
17. R. A. Street, P. Qi, R. Lujan, and W. S. Wong, "Reflectivity of disordered silicon nanowires," Appl. Phys. Lett. **93**, 163109 (2008).
18. Z. Fan, H. Razavi, J. Do, A. Moriwaki, O. Ergen, Y. Chueh, P. W. Leu, J. C. Ho, T. Takahashi, L. A. Reichertz, S. Neale, K. Yu, M. Wu, J. W. Ager, and A. Javey, "Three-dimensional nanopillar-array photovoltaics on low-cost and flexible substrates," Nat. Mater. **8**, 648–653 (2009).
19. R. E. Camacho, A. R. Morgan, M. C. Flores, T. A. McLeod, V. S. Kumsomboone, B. J. Mordecai, R. Bhattacharjea, W. Tong, B. K. Wagner, J. D. Flicker, S. P. Turano, and W. J. Ready, "Carbon nanotube arrays for photovoltaic applications," JOM **59**, 39–42 (2007).
20. T. Xu, S. Yang, S. V. Nair, and H. E. Ruda, "Nanowire-array-based photonic crystal cavity by finite-difference time-domain-calculations," Phy. Rev. B **75**, 125104 (2007).
21. S. Yamashita, Y. Inoue, S. Maruyama, Y. Murakami, H. Yaguchi, M. Jablonski, and S. Y. Set, "Saturable absorbers incorporating carbon nanotubes directly synthesized onto substrates and fibers and their applications to mode-locked fiber lasers," Opt. Lett. **29**, 1581–1583 (2004).
22. G. Chen, J. Wu, Q. Lu, H. R. Gutierrez, Q. Xiong, M. E. Pellen, J. S. Petko, D. H. Werner, and P. C. Eklund, "Optical antenna effect in semiconducting nanowires," Nano Lett. **8**, 1341–1346 (2008).
23. L. Hu and G. Chen, "Analysis of optical absorption in silicon nanowire arrays for photovoltatic applications," Nano Lett. **7**, 3249–3252 (2007).
24. J. Zhu, Z. Yu, G. F. Burkhard, C. M. Hsu, S. T. Connor, Y. Xu, Q. Wang, M. McGehee, S. Fan, and Y. Cui, "Optical absorption enhancement in amorphous silicon nanowire and nanocone arrays," Nano Lett. **9**, 279–282 (2009).
25. F. J. Garcia-Vidal, J. M. Pitarke, and J. B. Pendry, "Effective medium theory of the optical properties of aligned carbon nanotubes," Phys. Rev. Lett. **78**, 4289–4292 (1997).
26. W. L*ü*, J. Dong, and Z. Li, "Optical properties of aligned carbon nanotube systems studied by the effective-medium approximation method," Phys. Rev. B **63**, 033401 (2000).
27. J. Maxwell-Garnett, "Colours in metal glasses and in metallic films," Philos. Trans. R. Soc. London, Ser. A **203**, 385–420 (1904).
28. O. L. Muskens, J. G. Rivas, R. E. Algra, E. P. A. A. Bakkers, and A. Lagendijk, "Design of light scattering in nanowire materials for photovoltaic applications," Nano Lett. **8**, 2638–2642 (2008).
29. A. Taflove and S. C. Hagness, *Computational Electrodynamics: The Finite-Difference Time-Domain Method* (Artech House, Norwood MA, 2000).
30. L. Henrard and P. Lambin, "Calculation of energy loss for an electron passing near giant fullerenes," J. Phys. B **29**, 5127 (1996).
31. L. G. Johnson and G. Dresselhaus, "Optical properties of graphite," Phys. Rev. B **7**, 2275 (1973).
32. A. Farjadpour, D. Roundy, A. Rodriguez, M. Ibanescu, P. Bermel, J. D. Joanopoulos, S. G. Johnson, and G. Burr, "Improving accuracy by subpixel smoothing in FDTD," Opt. Lett. **31**, 2972–2974 (2006).
33. F. Pedrotti, L. Pedrotti, and L. Pedrotti, *Introduction to Opitcs* (Pearson Education, New Jersey, 2007).
34. S. Redmond, S. Rand, X. Ruan, and M. Kaviany, "Multiple scattering and nonlinear thermal emission of Yb^{3+},Er^{3+}:Y_2O_3 nanopowders," J. Appl. Phys. **95**, 4069–4077 (2004).
35. X. Ruan and M. Kaviany, "Photon localization and electromagnetic field enhancement in laser irradiated, random porous media," Microscale Thermophys. Eng. **9**, 63–84 (2005).
36. X. Ruan and M. Kaviany, "Enhanced nonradiative relaxation and photoluminescence quenching in random, doped nanocrystalline powders," J. Appl. Phys. **97**, 104331–1–8) (2005).
37. C. Lin and M. L. Povinelli, "Optical absorption enhancement in silicon nanowire arrays with a large lattice constant for photovoltaic applications," Opt. Express **17**, 19371 (2009).
38. T. W. Ebbesen, H. J. Lezec, H. F. Ghaemi, T. Thio, and P. A. Wolff, "Extraordinary optical transmission through sub-wavelength hole arrays," Nature **391**, 667–669 (1998).
39. J. Li, H. Yu, S. M. Wong, G. Zhang, X. Sun, P. G. Lo, and D. Kwong, "Si nanopillar array optimization on Si

#122794 - $15.00 USD Received 15 Jan 2010; revised 23 Feb 2010; accepted 3 Mar 2010; published 12 Mar 2010

1. Introduction

Ever since large-scale aligned CNT arrays have been synthesized [1], they have exhibited promise for various applications. In particular, many interesting optical properties have been observed in aligned carbon nanotube arrays, such as photonic crystal effects [2–4], directional emission [5–7], wavelength-selective emission and polarization-dependent reflection [8, 9], and high absorptivity [10, 11].

Optical properties of CNT arrays depend first on the atomic structure of each individual CNT and then on their collective arrangement. For an individual CNT, the optical properties of single-walled (SW) CNTs and MWCNTs should be considered separately. The optical properties of SWCNTs, especially those with diameters less than 1 nm, exhibit very strong dependence on the detailed atomic structure (chirality) [12–14]. Chirality-controlled CNT growth or chirality separation is still difficult in experiments. Thus SWCNT arrays usually contain many different chiralities with a random distribution, which complicates the engineering of optical properties and functionalities. In contrast, MWCNTs, due to their larger size, have more regular and uniform optical properties [15]. It is thus reasonable to treat each MWCNT as a homogeneous medium [4] and design the structure for different applications.

The optical properties of a CNT array further depend on the manner in which the CNTs are arranged, including pattern and intertube distance. Vertical arrays of nanotubes and nanowires have attracted much attention recently in solar [16–19], photonic crystal [20], mode-locked fiber lasers [21], and nanoantenna [22] applications. For example, absorption enhancement in silicon nanowire arrays has been predicted [23] using electromagnetic (EM) calculations and observed in experiments [24]. Also, anisotropic optical scattering is predicted and observed for an individual semiconductor nanowire [22]. In comparison, MWCNT arrays possess a similar cylinder array structure. Although enhanced absorption [10] and anisotropic scattering [6] are experimentally observed, they have been less investigated theoretically, and quantitative analysis is still lacking.

Most theoretical studies simply treat CNT array as a homogeneous medium [25, 26] using the Maxwell-Garnett theory (MGT) [27], which provides a qualitative understanding of optical properties. For example, using this theory, the extremely dark property of CNT array is attributed to the very small dielectric contrast at the air and CNT array interface [10]. However, MGT clearly oversimplifies the problem because various structural features of the array are simply represented by volume fraction. Some important phenomena, such as field enhancement and multiple scattering [28] are thus neglected within this homogeneous medium approach. Recently, Lidorikis *et al.* carried out FDTD calculations for infinitely long MWCNT arrays with irradiation incident from one side of the array [4]. They predicted the CNT arrays to be good absorbers in the visible band and photonic crystals in ultraviolet band. They focus on infinitely long tubes, and the electric field is polarized parallel to the tube axis. In contrast, when irradiation is incident from the top of the vertical array, the physical process is much different. Three-dimensional simulations are needed, and different polarizations should be considered.

In this work, we treat an individual MWCNT as a solid anisotropic cylinder with an effective dielectric tensor. Ordered vertically aligned CNT arrays are investigated with top-side irradiation. A FDTD method [29] is used to calculate the reflection, transmission, and absorption properties of MWCNT arrays. Different intertube distances, tube lengths and diameters, and different incident wavelengths, angles, and polarizations are considered. The findings are discussed and compared with experimental results and predictions from MGT.

#122794 - $15.00 USD Received 15 Jan 2010; revised 23 Feb 2010; accepted 3 Mar 2010; published 12 Mar 2010

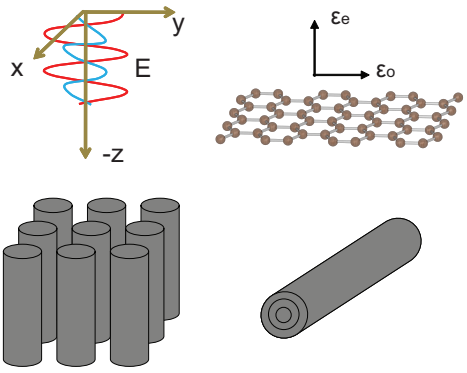

Fig. 1. (Color online) Left: A sketch of a CNT array subject to normal incidence. Upper right: single layer graphite and the anisotropic dielectric tensor. Lower right: MWCNT as a roll of multilayer graphite.

2. Methods

A general schematic of the ordered vertical array of MWCNTs considered in this work is shown in Fig. 1. CNTs are aligned along the z direction, and the array forms a 2D square lattice in the xy plane. The surrounding medium is simply air. Normal or oblique incidence illuminates the array from the top. In our calculations, a CNT is treated as a roll of graphite with a local dielectric tensor given by [30]

$$\varepsilon(\hat{r},\hat{\phi},\hat{z}) = \varepsilon_e \hat{r}\hat{r} + \varepsilon_o(\hat{z}\hat{z} + \hat{\phi}\hat{\phi}), \tag{1}$$

where $\hat{r},\hat{\phi},\hat{z}$ are the base vectors of the cylindrical coordinate system, and $\varepsilon_e, \varepsilon_o$ are the dielectric function of graphite for the extraordinary and ordinary rays, respectively. Clearly, this dielectric tensor has non-diagonal components in Cartesian coordinates, which makes it difficult to be applied in FDTD calculations. It is thus further simplified to a diagonalized form within the effective medium approximation. The components of the dielectric tensor are then given by [26]

$$\begin{aligned} \varepsilon_{\parallel} &= \varepsilon_o \\ \varepsilon_{\perp} &= \sqrt{\varepsilon_e \varepsilon_o}. \end{aligned} \tag{2}$$

where $\varepsilon_{\parallel}$ and $\varepsilon_{\perp}$ are the components of the dielectric tensor parallel and perpendicular to the CNT axis, respectively. We adopt the graphite properties from Ref. [31] and calculate the dielectric tensor of an individual CNT using Eq. (2). The results are shown in Fig. 2.

Once the dielectric tensor of an individual CNT is obtained, the FDTD method, implemented in the Meep package [32], is employed to obtain reflectance, transmittance, and absorbance of CNT arrays. A spatial resolution Δx of 5 nm is selected based on convergence tests, and the time step is $\Delta t = 0.5\Delta x/c$, where c is the speed of light. Periodic boundary conditions are applied in both x and y directions of the simulation domain, so that a unit cell with only one CNT is needed to model the infinitely large CNT array. Narrow-band Gaussian pulses centered at different frequencies are generated at the incidence plane, and Fourier transforms are applied to calculate the energy flux at each central frequency. Because nonlinear effects are not included in numerical calculations, components at other frequencies in the Gaussian pulse do not affect the energy flux at the central wavelength. The incident frequencies correspond to wavelengths from 400 to 850 nm.

#122794 - $15.00 USD Received 15 Jan 2010; revised 23 Feb 2010; accepted 3 Mar 2010; published 12 Mar 2010

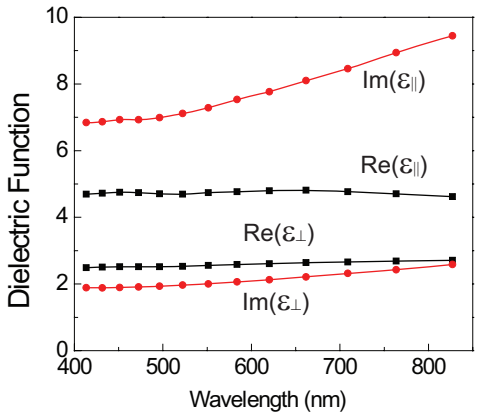

Fig. 2. (Color online) Effective dielectric function of an individual CNT.

As stated above, MGT has been used as a simpler method to predict the optical properties of CNT arrays in many prior studies. In this work we also use MGT to obtain radiative properties, and then compare the results to those of FDTD simulations. Different from our cylinder array model, MGT treats the CNT array entirely as an effective homogeneous medium. Because the CNTs are anisotropic and aligned along a particular direction, the effective medium is optically anisotropic. The components of the effective dielectric tensor of such a medium with CNT volume fraction f are given by

$$\begin{aligned} \varepsilon_{eff\parallel} &= 1+f(\varepsilon_{\parallel}-1) \\ \varepsilon_{eff\perp} &= 1+\frac{f(\varepsilon_{\perp}-1)}{1+\frac{1}{2}(\varepsilon_{\perp}-1)(1-f)} \end{aligned} \tag{3}$$

where $\varepsilon_{eff\parallel}$ and $\varepsilon_{eff\perp}$ are the components parallel and perpendicular to the CNT direction, respectively. These equations are equivalent to Eqs. (7) and (8) in Ref. [25]. Thermal radiative properties of such homogeneous mediums can be calculated by analytical methods, which involve calculating multiple reflections between the upper and lower surfaces. Here for convenience we simply perform FDTD calculations on these media and obtain the reflectance, transmittance, and absorbance. The results obtained in this way are denoted by "MGT" in the following sections.

3. Results and discussion

The structure of a nanotube array is characterized by many parameters, which can be consolidated to tube diameter, intertube distance, and tube length for two-dimensional square lattice. Intertube distance and tube diameter are sometimes combined to define the volume fraction. In our calculations, the typical diameters of MWCNTs are from 40 to 240 nm, the intertube distances vary from 200 to 600 nm, and the tube lengths are from 1 μm to 3 μm. Very long CNTs are approximated by truncating the CNTs using a perfectly matched layer (PML). In addition, different incident angles are considered. The following subsections consider how these parameters affect the optical properties of the CNT arrays. The effects of each parameter are investigated while others are fixed. Four parameters are discussed in sequence: volume fraction, tube length, tube diameter, and incident angle.

#122794 - $15.00 USD Received 15 Jan 2010; revised 23 Feb 2010; accepted 3 Mar 2010; published 12 Mar 2010

3.1. *Volume fraction*

To study volume fraction, the CNT diameter is chosen to be 80 nm, and the tube length is 1 μm. Different intertube distances from 200 to 400 nm are considered, and the corresponding volume fraction f ranges from 0.126 to 0.031. The calculated results for total reflectance, transmittance, and absorbance of CNT arrays subjected to normal incidence are shown in Fig. 3. As indicated in the figure, the reflectance is generally very small; even when the volume fraction is as large as 0.126, the maximum reflectance is less than 0.5%. The low reflection is primarily due to the large open area of the CNT array that allows light to enter easily. Low reflection has also been observed in other nanoscale cylinder array structures such as silicon nanowire arrays [23]. The present CNT arrays exhibit even smaller reflectance, because CNTs have smaller real and imaginary parts of the dielectric function and thus less reflectance compared with silicon. The calculated wavelength-dependent reflectance exhibits some oscillation, which is due to the interference between the reflected waves at the top and back surfaces. Also, the reflectance decreases with decreasing volume fraction, which can be attributed to the smaller CNT frontal area when the volume fraction is small.

Because the reflectance R is small, the transmittance T is almost completely determined by the absorbance A ($T = 1 - A - R$). Our calculations show that absorbance decreases with smaller volume fractions. This can be easily understood considering that CNTs are the only absorbers and fewer CNTs make the array less absorptive. Another interesting feature is that the absorbance of the CNT arrays decreases with increasing incident wavelength.

This wavelength dependence can be understood by considering how an individual CNT absorbs light. The absorption α is generally related to the incident wavelength λ and the imaginary part of the refractive index κ by [33]

$$\alpha = \frac{4\pi\kappa}{\lambda}. \tag{4}$$

κ can be derived from the dielectric function,

$$\kappa = \sqrt{\frac{\sqrt{\varepsilon_1^2 + \varepsilon_2^2} - \varepsilon_1}{2}}, \tag{5}$$

where ε_1 and ε_2 are the real and imaginary parts of the dielectric function, respectively. When the irradiation is directly from the top, the electric field is always perpendicular to the tube axis, and $\varepsilon_\perp$ should be used to evaluate κ. As shown in Fig. 1, $\varepsilon_\perp$ has very small dependence on wavelength, so κ is also nearly invariant with wavelength. The absorption of an individual CNT will thus decrease with wavelength. The present results indicate that the absorbance of CNT arrays exhibit a similar wavelength dependence as an individual CNT. As shown later, such a wavelength dependence remains valid when the intertube distance is less than the incident wavelength. The conclusion cannot be extended to the cases when the intertube distance is larger than the incident wavelength.

For comparison, the optical properties for $f = 0.126$ and 0.031 calculated from MGT are also shown in Fig. 3. Compared to the FDTD results, both reflectance and absorbance evaluated using MGT are smaller for same volume fraction. For example, when the volume fraction is 0.031, MGT underestimates the absorbance by up to 50% at 413 nm incidence. This finding suggests that nanoscale inhomogeneities within the cylinder array structure are important to its optical properties. As shown in the inset of Fig. 3b, the field distribution is not uniform in the cross section perpendicular to the propagation direction. Possible multiple scattering of light within the cylinder array structure is captured in our calculation but not in the homogeneous medium treatment. Multiple scattering can elongate the optical path of photons and result

#122794 - $15.00 USD Received 15 Jan 2010; revised 23 Feb 2010; accepted 3 Mar 2010; published 12 Mar 2010

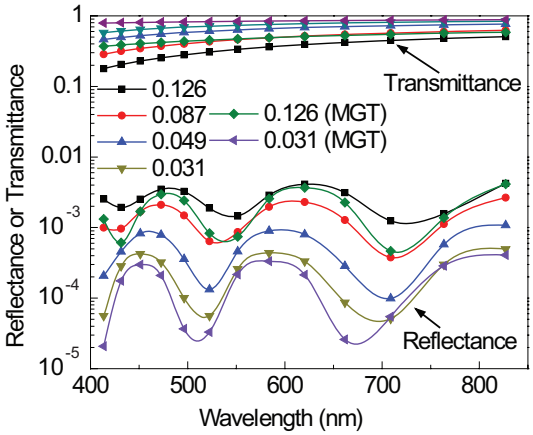

(a) Reflectance and Transmittance

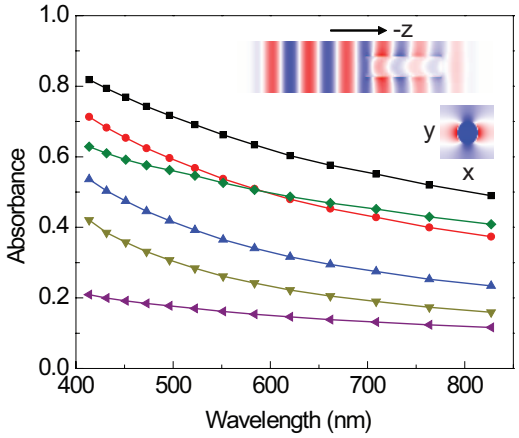

(b) Absorbance

Fig. 3. (Color online) (a) Reflectance and transmittance and (b) absorbance of the CNT array from FDTD calculation and MGT with different volume fractions. The reflectance and transmittance are shown in a log scale plot. Insert: an instant electric field distribution of the cross sections of the simulation domain with 500 nm incident wavelength and 0.126 volume fraction. The upper figure is scaled in the vertical direction for clarity.

#122794 - $15.00 USD Received 15 Jan 2010; revised 23 Feb 2010; accepted 3 Mar 2010; published 12 Mar 2010

in field enhancement, which greatly enhances absorption [34–36]. Also, for normal incidence the $\varepsilon_{\|}$ component does not contribute to absorption in the MGT treatment, since the electric field is always perpendicular to the tube axis in this homogeneous medium approximation [see Eq. (3)]. In FDTD, however, because the CNT array is not homogeneous, the wavefront is no longer a plane, as shown in the inserted figure in Fig. 3. Diffraction can induce an electric field component parallel to the tube axis, so the large $\varepsilon_{\|}$ component can also contribute to the absorption. Besides absorption, enhanced reflectance as compared MGT is also evident in our results. This enhancement can also be attributed to the multiple scattering which increases the chance of back-scattering as well. Both enhanced absorption and reflection indicate that multiple scattering significantly decreases transmission in FDTD treatment as compared in MGT, as expected.

3.2. Length effect

CNTs with various lengths from less than one micron to a few hundred micron can be fabricated in the experiments. To analyze the length effect, CNT lengths of 1-3 μm have been simulated by the FDTD method. Direct simulation of even longer CNTs requires substantially computational time and is not practical for electromagnetic calculations. An exception is that the reflectance of semi-infinite CNTs can be calculated by using the PML to truncate the simulation domain. PML is an artificial material used in FDTD calculations: the EM waves entering the PML will be completely absorbed and nothing is reflected. Applying this boundary condition at the back surface is equivalent to the semi-infinite case. The calculated reflectance and absorbance of CNT arrays with different lengths (diameter of 80 nm and intertube distances of 400 nm, $f = 0.031$) are shown in Fig. 4. The results indicate that the reflectance profiles for different tube lengths all exhibit oscillations with the wavelength due to the interference. Longer tubes produce smaller oscillation amplitudes because the reflection from the bottom surface becomes weaker. The average reflectance for different lengths does not differ significantly from each other, and they are all oscillating around the reflectance value of the case using PML. Absorption data in Fig. 4 clearly indicate that longer tubes have higher absorbance. The absorbance of infinitely long tubes is very close to unity, because they simply have $A = 1 - R$. The length-dependent absorbance at any wavelength can be well-fitted to the form $A(L) = 1 - \exp(-\alpha L)$, where α is the absorption coefficient and L is the tube length, indicating that the field entering the CNT array follows a similar exponential decay as in homogeneous materials. In experiments, if the tubes are sufficiently long, only the top surface can slightly reflect light, so the CNTs appear dark [7, 10]. If the tubes are relatively short, the reflection from the back surface and the substrate is considerable, and hence the CNT arrays can appear shiny [8].

3.3. Effects of tube diameter and intertube distance

To study how the diameter and intertube distance (or more generally, periodicity) affect the optical properties, we investigate different CNT arrays with a fixed volume fraction of 0.126. The tube diameter varies from 40 to 240 nm, corresponding to periodicity from 100 to 600 nm. The tube length is either fixed as 1 μm, or assumed to be semi-infinite (denoted by "inf"). The results of FDTD calculations, together with those from MGT, are shown in Fig. 5. Because the incident wavelength ranges from 400 to 850 nm, the intertube distances of 100 and 400 nm lie in the sub-wavelength regime. In comparison, the 600 nm intertube distance is larger than some incident wavelengths and smaller than others. The relationship between periodicity and incident wavelength is important because the results indicate that optical properties of CNT arrays exhibit two distinctly different regions. For intertube distances less than the wavelength, the reflectance increases with larger periodicity, and at each periodicity it exhibits some oscillation around the semi-infinite value. At the same time, the absorbance of 1 μm CNT array increases

#122794 - $15.00 USD Received 15 Jan 2010; revised 23 Feb 2010; accepted 3 Mar 2010; published 12 Mar 2010

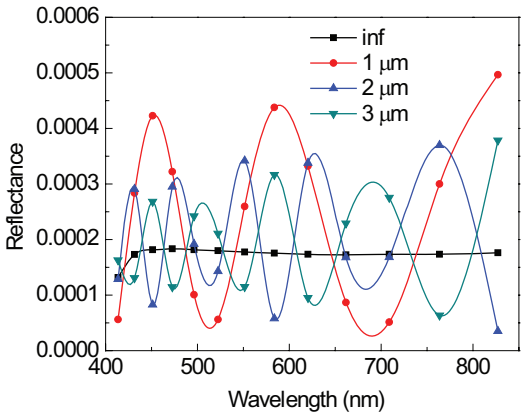

(a) Reflectance

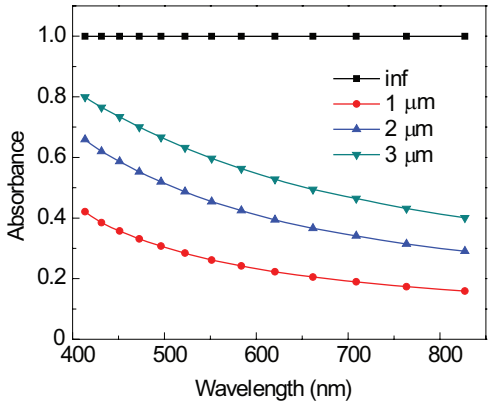

(b) Absorbance

Fig. 4. (Color online) (a) Reflectance and (b) absorbance of CNTs with different lengths. "Inf" indicates that the back tip of CNT extends into a PML, which approximates semi-infinite CNTs.

with periodicity and at each periodicity the absorbance decreases with larger wavelength. Similar results are also obtained for silicon nanowire arrays with finite lengths [37]. The MGT homogeneous medium, which can be viewed as an infinitesimal tube diameter and periodicity, gives the lower limit of both reflectance and absorbance. The semi-infinite reflectance is small and nearly independent of the wavelength. The semi-infinite absorbance is thus almost 100% in the entire visible range.

In contrast, for 600 nm intertube distance, abnormal behavior for both reflectance and absorbance is seen. For both 1 μm long and semi-infinite CNT arrays, the reflectance is significantly larger when the incident wavelength is smaller than 600 nm. The wavelength dependence does not show a simple oscillation in this region. Also, the absorbance increases with wavelength when the wavelength is smaller than 600 nm. Note that the large reflectance and small absorbance are not correlated, because the increment of reflectance is still very small compared with change in absorbance. An absorbance maximum appears when periodicity is equal to the

#122794 - $15.00 USD Received 15 Jan 2010; revised 23 Feb 2010; accepted 3 Mar 2010; published 12 Mar 2010

wavelength, indicating that a minimum in transmission occurs at the same wavelength. Similar results have been reported in transmission experiments on nanohole arrays [38]. The relative invariance of absorbance with wavelength for 600 nm periodicity is due to a combined effect of the dielectric function of individual CNTs and scattering. The dielectric function is almost independent of wavelength, so that the maximum scattering creates a maximum absorption at 600 nm. In the wavelength regime includes this maximum, the absorbance appears wavelength-independent.

Although some interesting features are apparent when the periodicity is larger than the incident wavelength, we will forgo additional analysis, because the periodicity of experimental CNT array is almost always smaller than visible wavelengths. Confining our discussion to sub-wavelength periodicities, it can then be concluded that for a fixed volume fraction both absorbance and reflectance increase with increasing periodicity. Simultaneously increases in absorption and reflection are not contradictory because for fixed tube lengths part of the incident light is transmitted. Increased absorption with periodicity is also seen in electromagnetic calculations of silicon nanopillar arrays and was explained by increased scattering: when the periodicity is near the incident wavelength, the scattering will increase, resulting in elongated optical paths and thus enhanced absorption [39].

3.4. Angular dependence

Although our calculations predict CNT arrays to have low reflectance at normal incidence, it is necessary to quantify variations from different incidence angles or tube misalignment. Angular-dependent reflectance and absorbance are thus investigated. Unlike the normal incidence case, transverse electric (TE) and transverse magnetic (TM) waves should be considered separately. Incident angles from 0^o to 70^o are considered. Larger angles are not considered due to the numerical difficulty. The polar angle is fixed at 0^o , following previous calculations for silicon nanowire arrays showing only small effects of polar angle [23]. Consequently, the projection of the incident ray on the *xy*-plane is always along the *x* direction. The tube diameter for the cases considered is 80 nm, the intertube distance is 200 nm, the tube length is 1 μm, and the incident wavelength is 500 nm. Trends for longer tube lengths are similar. The calculated angular dependent reflectance and absorbance are compared with the MGT and shown in Fig. 6.

For a general homogeneous medium, the reflectance of the TE wave increases with angle monotonically to 100%. Conversely, the reflectance of TM wave decreases to 0 at the Brewster angle and then increases to 100% at 90^o . The predicted reflectance by MGT matches this trend. In contrast, the FDTD results for the CNT array show that the reflectance of both TE and TM waves first decreases slightly at small angles and finally becomes very large. This indicates that compared to normal incidence, a non-zero incident angle or small misalignment of the CNTs can further reduce the reflectance. Also, the reflectance of TE waves oscillates and drops to a local minimum near 50^o, which is likely due to the antenna effect. One effect that can be resolved by both FDTD and MGT is larger reflectance of TM waves as compared to TE waves at large angles. This phenomenon is due to the TM wave's electric field component along the tube axis that causes higher reflection.

The angular-dependent absorbance of TE waves increases with incident angle in the range considered. For TM waves, the absorbance reaches a maximum near 50^o and then decreases. MGT predicts similar trends but smaller values due to the neglect of scattering under the homogeneous medium assumption. To understand angular-dependent absorption, two angular regions should be considered separately. When the incident angle is small, the reflectance is negligible and almost all incident light can enter the medium. The absorption increases with incident angle due to the longer paths. When the angle is large, reflectance starts to increase

#122794 - $15.00 USD Received 15 Jan 2010; revised 23 Feb 2010; accepted 3 Mar 2010; published 12 Mar 2010

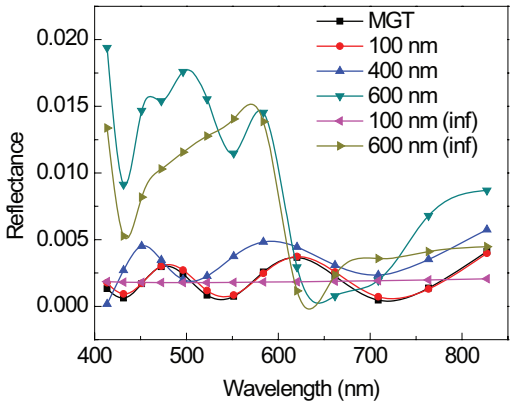

(a) Reflectance

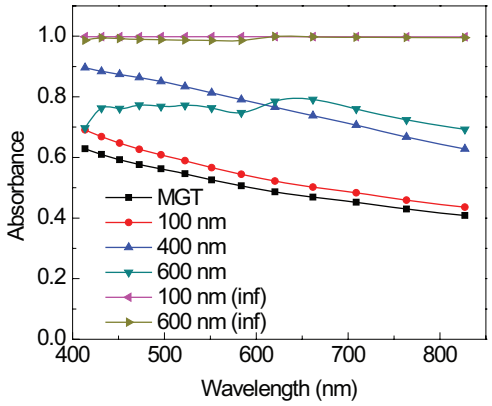

(b) Absorbance

Fig. 5. (Color online) (a) Reflectance and (b) absorbance of CNT arrays with different periodicity. The volume fractions are fixed as 0.126. "Inf" denotes the semi-infinite reflectance or absorbance.

dramatically. Although the optical path becomes longer, less light can enter the medium because of the large reflectance. The competition of increasing reflection and increasing optical path gives the maximum in the absorbance curve for TM wave near 50º. The absorbance of TE waves does not show a maximum only because it is difficult to perform similar calculations at very large incident angles. In fact, a maximum absorption angle is still expected because the reflectance will eventually become 100% for 90º incidence, and the absorbance will drop to zero.

3.5. Discussion on optimizing dark materials

Using a low-density, thin MWCNT array, Yang *et al.* [10] achieved the darkest material ever reported. The CNT array density in their experiment is as low as 0.01-0.02 g/cm^3 with diameters of only 8-11 nm. The sample thickness is a few hundred micron and comparable to our semi-infinite case. The minimum reported reflectance was 0.07% to 0.045% from 457 to 633

#122794 - $15.00 USD Received 15 Jan 2010; revised 23 Feb 2010; accepted 3 Mar 2010; published 12 Mar 2010

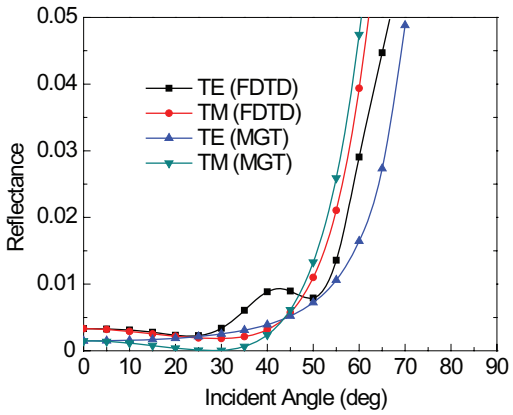

(a) Reflectance

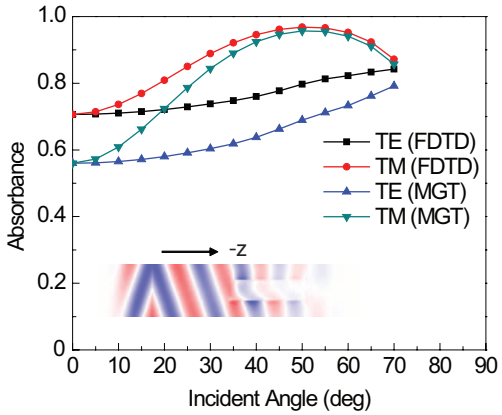

(b) Absorbance

Fig. 6. (Color online) (a) Reflectance and (b) absorbance of CNTs at different incident angle. Insert: an instant field distribution for TE wave under 20° oblique incidence. The figure is scaled in the vertical direction for clarity.

nm incidence light. In comparison, our FDTD calculations with a 0.031 volume fraction and a density of 0.06 g/cm^3 predict a reflectance of 0.02% (semi-infinite reflectance in Fig. 4). The results in general agree quite well, and the discrepancy is in that lower volume fraction (lower density) in Ref. [10] should give smaller reflection. One note is that experiments are complicated by the rough top surface of the array structure, as sketched in Fig. 7. The roughness due to variable nanotube length shown in Fig. 7(a) will reduce reflectance, while the roughness due to nanotube tip bending as shown in Fig. 7(b) will increase reflectance because of higher local volume fraction and larger parallel dielectric function. How surface roughness affects reflectance depends on which mechanism dominates. The tip bending is difficult to avoid for thin CNTs because of their low bending modulus. Our calculations suggest that even if much thicker tubes (80 nm in diameter) are used, very small reflection can still be achieved under good alignment. Therefore, to further improve the darkness of CNT arrays, methods for improving the verticality of the CNT tips while allowing variability in tube length should be pursued.

Also, the angular dependence predicted in the present work suggests that a directional emis-

#122794 - $15.00 USD Received 15 Jan 2010; revised 23 Feb 2010; accepted 3 Mar 2010; published 12 Mar 2010

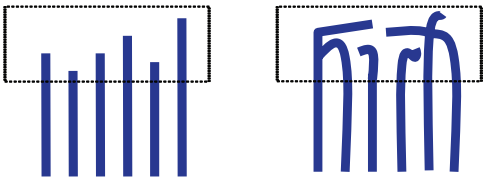

(a) (b)

Fig. 7. A sketch of surface roughness of CNT array. (a): aligned CNT array with random tube length. (b): aligned CNT array with tip bending.

sion effect may exist. Our calculation only shows angular dependent total reflection. For the antenna application, far field optical scattering should also be further investigated using computational EM methods to compare with the experimental results in Refs. [6] and [7].

4. Summary

In summary, the optical properties of MWCNT array within sub-wavelength arrays periodicities are numerically studied. The results indicate that such CNT arrays can have very low reflectance and relatively high absorbance over the entire visible band. With a higher volume fraction, CNT arrays will exhibit larger absorbance but also higher reflectance. Variations of CNT length reveal that the light within the array experiences an exponential decay similar to that in normal homogeneous materials. With the same volume fraction, thicker CNTs with larger intertube distance will generally reflect more light but also absorb the light more efficiently per unit tube length. Angular dependence calculations show that when the incident angle is as large as 50^o, the CNTs can still produce very small reflectance for both TE and TM waves. This indicates that a small misalignment of the CNT array will not substantially affect the absorption performance of CNT arrays.

Acknowledgments

This work is partially supported by the Air Force Office of Scientific Research through the Discovery Challenge Thrust (DCT) Program (Grant No.FA9550-08-1-0126, Program Manager Joan Fuller). XLR acknowledges the faculty startup funds from Purdue University. Fruitful discussions with John Zuidema and Aaron Sisto are gratefully appreciated. HB is also grateful to Dr. Dan Jiao, Jianfang Zhu, and Jian Wang for their help on the FDTD calculations.

#122794 - $15.00 USD Received 15 Jan 2010; revised 23 Feb 2010; accepted 3 Mar 2010; published 12 Mar 2010